Molecular Cell, Vol. 3, 11–21, January, 1999, Copyright ©1999 by Cell Press

Altered Trafficking of Lysosomal Proteins in Hermansky-Pudlak Syndrome Due to Mutations in the β3A Subunit of the AP-3 Adaptor

Esteban C. Dell'Angelica,* Vorasuk Shotelersuk,† Ruben C. Aguilar,* William A. Gahl,† and Juan S. Bonifacino*‡
*Cell Biology and Metabolism Branch
†Heritable Disorders Branch
National Institute of Child Health and Human Development
National Institutes of Health
Bethesda, Maryland 20892

Summary

Hermansky-Pudlak syndrome (HPS) is a genetic disorder characterized by defective lysosome-related organelles. Here, we report the identification of two HPS patients with mutations in the β3A subunit of the heterotetrameric AP-3 complex. The patients' fibroblasts exhibit drastically reduced levels of AP-3 due to enhanced degradation of mutant β3A. The AP-3 deficiency results in increased surface expression of the lysosomal membrane proteins CD63, lamp-1, and lamp-2, but not of nonlysosomal proteins. These differential effects are consistent with the preferential interaction of the AP-3 μ3A subunit with tyrosine-based signals involved in lysosomal targeting. Our results suggest that AP-3 functions in protein sorting to lysosomes and provide an example of a human disease in which altered trafficking of integral membrane proteins is due to mutations in a component of the sorting machinery.

Introduction

Integral membrane proteins destined for localization to the plasma membrane and compartments of the endosomal–lysosomal system begin their journey through the cell by being cotranslationally inserted into the membrane of the endoplasmic reticulum (ER) (High and Laird, 1997). The newly synthesized proteins undergo folding and other posttranslational modifications in the ER before being delivered to their final destinations. Sorting of these proteins largely depends on specific signals contained within their cytosolic domains. The sorting signals interact with components of membrane-bound organellar coats, which results in concentration of the integral membrane proteins into coated vesicles (Schekman and Orci, 1996; Rothman and Wieland, 1996; Kirchhausen et al., 1997). Many human diseases arise from mutations in integral membrane proteins that prevent them from reaching their ultimate cellular destinations. Most often, these mutations cause misfolding and retention of the newly synthesized proteins in the ER, followed by proteasome-mediated degradation (reviewed by Bonifacino and Weissman, 1998). Such is the fate, for example, of the mutant cystic fibrosis transmembrane conductance regulator in most cystic fibrosis patients (Ward et al., 1995; Jensen et al., 1995). The mutations can also disrupt the cytosolic sorting signals, as is the case for endocytosis-defective low-density lipoprotein receptors in patients with familial hypercholesterolemia (Davis et al., 1986). In the present study, we describe the first example of a human disease in which misrouting of integral membrane proteins is caused by mutations in a component of an organellar coat involved in protein sorting.

Our studies concern the Hermansky-Pudlak syndrome (HPS), an autosomal recessive disorder characterized by oculocutaneous albinism and platelet storage pool deficiency (Hermansky and Pudlak, 1959). These abnormalities arise from defects in specialized cytoplasmic organelles, namely melanosomes and platelet-dense granules. Over time, some HPS patients develop pulmonary fibrosis and granulomatous colitis, presumably due to accumulation of undegraded materials in lysosomes of reticuloendothelial cells. All the organelles affected in HPS contain lysosomal proteins and are therefore considered to be biogenetically related to lysosomes (Orlow, 1995; Israels et al., 1996). Thus, HPS could result from mutations in genes involved in the biogenesis of lysosome-related organelles.

A gene that is mutated in a subset of HPS patients has recently been identified by positional cloning (Oh et al., 1996). The gene, now termed *HPS1*, encodes a novel ubiquitously expressed protein of unknown function. Some HPS patients, however, do not have mutations in *HPS1* (Hazelwood et al., 1997). A clue to other genes that might be defective in HPS was provided by the discovery that the *Drosophila* pigmentation gene *garnet* encodes the δ subunit of the AP-3 adaptor complex (Ooi et al., 1997; Simpson et al., 1997). Altered expression of AP-3 δ mRNA was associated with abnormal pigment granules that, like mammalian melanosomes, are related to lysosomes (Ooi et al., 1997). AP-3 is a protein complex consisting of four ubiquitous subunits termed δ, β3A, μ3A, and σ3 (A or B isoforms) (Dell'Angelica et al., 1997a, 1997b; Simpson et al., 1997; reviewed by Odorizzi et al., 1998). Neuronal-specific isoforms of the β3A and μ3A subunits have been described (Pevsner et al., 1994; Newman et al., 1995). Like the related adaptor complexes AP-1 and AP-2, AP-3 interacts with the scaffolding protein clathrin (Dell'Angelica et al., 1998) and with sorting signals of integral membrane proteins (Ohno et al., 1996; Dell'Angelica et al., 1997a; Höning et al., 1998).

The above information led us to investigate whether some patients with HPS could have defects in AP-3. To this end, we screened a panel of fibroblast cultures from HPS patients and identified two siblings whose fibroblasts displayed drastically reduced levels of all four AP-3 subunits. The primary defect was the presence of compound heterozygous mutations in the β3A sub-

‡To whom correspondence should be addressed (e-mail: juan@helix.nih.gov).

unit. One of the mutant alleles (Δ390–410) encoded a protein with a 21-amino acid internal deletion, and the other ($L^{580}R$) encoded a protein with a nonconservative amino acid substitution. The mutations resulted in enhanced degradation of newly synthesized β3A with concomitant destabilization of other AP-3 subunits. The AP-3 deficiency in the patients' fibroblasts was associated with increased surface expression of the lysosomal membrane proteins CD63, lamp-1, and lamp-2, but not of nonlysosomal membrane proteins. The specific effect of AP-3 deficiency on the trafficking of lysosomal membrane proteins correlated with selective interaction of the μ3A subunit of AP-3 with tyrosine-based sorting signals of lysosomal proteins such as CD63 and lamp-1. These findings suggest that the mammalian AP-3 complex is involved in the sorting of integral membrane proteins to lysosomes and that impairment of this process may underlie the clinical symptoms of HPS.

Results

Defective Expression of AP-3 in Two Patients with HPS

Primary fibroblast cultures were established from skin biopsies of normal individuals and 20 patients diagnosed with HPS. Two patients were homozygous for a 16 bp duplication in the *HPS1* gene (Oh et al., 1996), while the others had no discernible mutations in this gene. The fibroblast cultures were examined by immunofluorescence microscopy using antibodies to the δ, β3, and σ3 subunits of the AP-3 complex. In fibroblasts from normal individuals, AP-3 exhibited a punctate cytoplasmic distribution (Figures 1A, 1D, and 1G), as previously reported (Dell'Angelica et al., 1997a; Simpson et al., 1997; Ooi et al., 1998). Cells from the patients with mutations in *HPS1* displayed a normal AP-3 staining pattern (Figures 1B, 1E, and 1H), indicating that inactivation of the HPS1 protein does not affect the overall distribution of AP-3. Sixteen of the remaining HPS patients also exhibited normal distribution of AP-3 in their fibroblasts (data not shown). However, two male siblings in this group (patients 40 and 42) displayed drastically reduced staining for AP-3, with only traces of the punctate structures being visible in some cells (Figures 1C, 1F, 1I, and data not shown). The two patients had normal distributions of two other adaptors, AP-1 and AP-2 (Figures 1L and 1O, respectively), thus suggesting that the defects were specific for AP-3.

We also performed immunoblot analyses of whole-cell extracts from the fibroblast cultures. We observed normal levels of all four AP-3 subunits in cells from the two patients with mutations in *HPS1* (e.g., P8 in Figure 2A), as well as from 16 patients without mutations in this gene (data not shown). In cells from patient 40 (P40, Figure 2A) and patient 42 (data not shown), however, δ and σ3 were decreased to 20%–30% and β3 and μ3 to <5% the levels found in normal cells. As controls, we examined the levels of the γ subunit of AP-1, the α subunit of AP-2, and of ARF (a small GTP-binding protein that regulates membrane association of AP-3 in vivo; Ooi et al., 1998). The amounts of these three proteins were similar in normal and patient 40 cells (Figure 2A), again suggesting that the defects detected in the two siblings were specific for AP-3.

The presence of detectable amounts of all four subunits of AP-3 in fibroblasts from patients 40 and 42 suggested that these cells could assemble a small amount of the complete complex. In support of this, the size distribution of the trace amount of β3A in fibroblasts from patient 40 was comparable to that of β3A in normal cells as inferred from analytical gel filtration (Figure 2B) and corresponded to the reported size of human AP-3 (Dell'Angelica et al., 1997a). As expected, the levels and elution profiles of the AP-2 α subunit from the gel filtration column were similar in the extracts from the normal individual and from patient 40 (Figure 2B).

Mutations in the AP-3 β3A Subunit

Northern analyses on total RNA revealed that fibroblasts from patient 40, a normal individual, and a patient with mutations in *HPS1* (patient 8) expressed equivalent levels of mRNAs for the AP-3 subunits δ, β3A, μ3A, σ3A, and σ3B (Figure 2C), as well as for μ3B, an isoform of μ3A expressed at very low levels in these cells (data not shown). The sizes of the AP-3 subunit mRNAs were also similar in cells from the three individuals. Thus, the decreased protein levels of AP-3 subunits in fibroblasts from patient 40 were not due to reduced transcript levels or the occurrence of large insertions/deletions.

We next sequenced cDNAs encoding the AP-3 subunits from patient 40. All the sequences were found to be normal, except for that of β3A, which was heterogeneous for a 63 bp deletion and a single nucleotide substitution (Figures 3A–3C). Identical mutations were found in β3A cDNA prepared from patient 42. The deletion and the point mutation occurred on different alleles, as demonstrated by direct sequencing of an RT-PCR product derived from the mRNA copy not having the deletion (data not shown) as well as by analyses of the segregation of the mutations among members of the patients' family. In the latter analyses, PCR-based assays demonstrated that the father and two apparently normal siblings carried the deletion mutant allele and a normal allele (Figures 3E and 3G, lanes 1, 5, and 6), whereas the mother had an allele with the point mutation and a normal allele (Figures 3E and 3G, lane 2). Only the two family members having mutations in both β3A alleles (i.e., patients 40 and 42) displayed HPS, thus confirming the recessive nature of the mutations. Taken together, these results indicated an association between the disease and the observed compound heterozygous mutations in β3A. The deletion allele encodes a protein lacking residues 390–410, whereas the point mutation results in a protein with the nonconservative substitution $L^{580}R$ (Figures 3A–3C).

Fate of β3A and σ3 in Fibroblasts from HPS Patient 40

The fate of mutant β3A was studied by pulse-chase analyses. The amounts of β3A synthesized after a 20 min pulse were similar in fibroblasts from patient 40 and from a normal individual (Figures 4A and 4B). Within the first hour of chase, in both the normal and patient's cells, the newly synthesized β3A protein underwent a

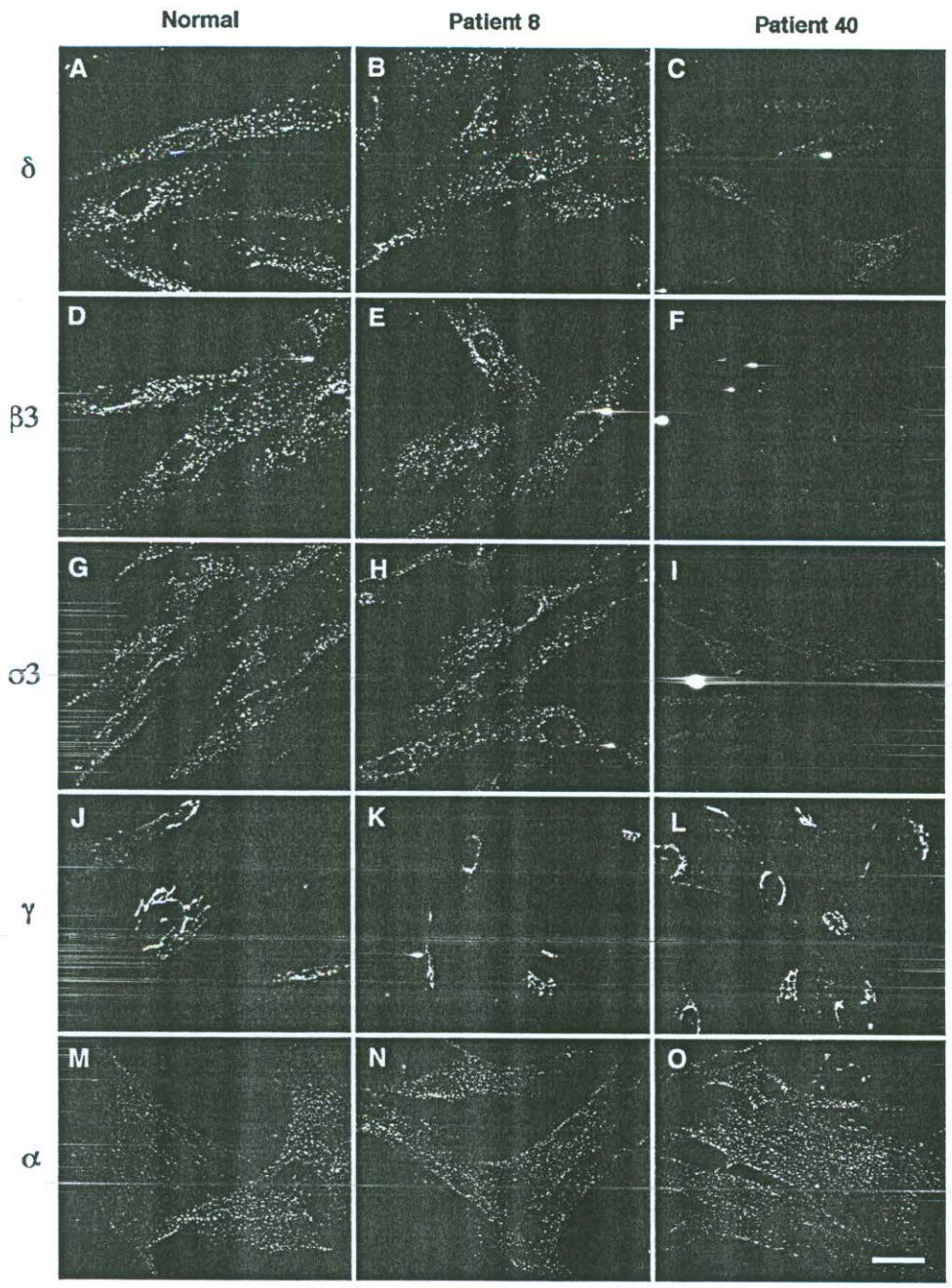

Figure 1. Immunofluorescence Microscopy Analysis of AP-3 Expression in Fibroblasts from a Normal Individual and from Two HPS Patients

Fibroblasts in primary culture from a normal individual (A, D, G, J, and M), a patient with mutations in *HPS1* (patient 8) (B, E, H, K, and N), and patient 40 (C, F, I, L, and O) were fixed, permeabilized, and incubated with primary rabbit antibodies to the δ (A–C), β3 (D–F), or σ3 (G–I) subunits of AP-3, the γ subunit of AP-1 (J–L), or the α subunit of AP-2 (M–O). The primary antibodies were revealed by incubation with either Cy3-conjugated anti-rabbit immunoglobulins (A–I) or Alexa448-conjugated anti-mouse immunoglobulins (J–O) secondary antibodies. Images were obtained by confocal fluorescence microscopy using identical parameters for the three cell samples. Notice the punctate cytoplasmic staining for AP-3 subunits in normal (A, D, and G) and patient 8 (B, E, and H) cells, and the absence of this pattern in patient 40 cells (C, F, and I). Bar, 20 μm.

posttranslational modification that resulted in increased electrophoretic mobility (Figure 4A, compare 0 and 1 hr chase times). This modification likely corresponded to the previously described serine-phosphorylation of β3A (Dell'Angelica et al., 1997b), since the mobility change could be reversed by treatment in vitro of the 1 hr chase samples with alkaline phosphatase (Figure 4C). Thus, the β3A mutations described here do not seem to affect either the protein's biosynthesis or its phosphorylation. On the other hand, the in vivo stability of mutated β3A was dramatically reduced (Figure 4A). Whereas the half-life of β3A in normal fibroblasts was greater than 16 hr,

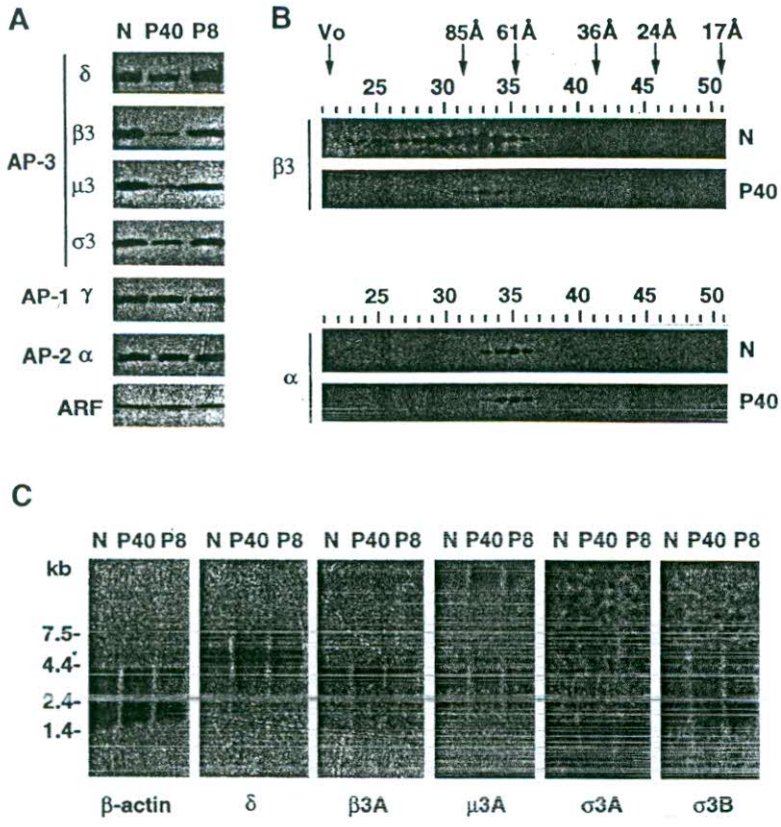

Figure 2. Expression Levels of AP-3 Subunits in Fibroblasts from HPS Patient 40 as Determined by Immunoblot or Northern Blot Analysis

(A) Fibroblast extracts from a normal individual (N), a patient with mutations in *HPS1* (P8), or patient 40 (P40) were resolved by SDS-PAGE and analyzed by immunoblotting with antibodies to the δ, β3, μ3, or σ3 subunits of AP-3, the γ subunit of AP-1, the α subunit of AP-2, or the small GTP-binding protein ARF, as indicated in the figure. Notice the reduced levels of all four subunits of AP-3 and the normal levels of AP-1 γ, AP-2 α, and ARF in cells from patient 40.

(B) Triton X-100 extracts of fibroblasts from a normal individual (N) and from patient 40 (P40) were fractionated on a Superose 6 gel-filtration column. The fractions were analyzed by immunoblotting for AP-3 β3 and AP-2 α. The positions of molecular size markers (Stokes' radii given in Ångstroms) and the void volume (Vo) are indicated. Despite the markedly different levels, β3 peaked at fractions #32–34 in both patient 40 and normal cells.

(C) Northern analyses showing normal expression of AP-3 subunit mRNAs in cells from patient 40. Total RNA extracted from fibroblasts from a normal individual (N), patient 8 (P8), or patient 40 (P40) were resolved on formaldehyde gels, transferred to nylon membranes, and probed with ^{32}P-labeled DNA probes to β-actin (control), δ, β3A, μ3A, σ3A, or σ3B, as indicated.

its half-life in fibroblasts from patient 40 was reduced to about 2.5 hr. The σ3 subunit was also synthesized at a normal rate and exhibited increased degradation, albeit to a lesser extent, in cells from patient 40 as compared to normal cells (Figure 4A). Degradation of β3A and σ3 could be partially inhibited with the proteasomal inhibitor, LLnL (Figure 4A). These results suggest that the mutated forms of β3A, as well as unassembled σ3, are more susceptible to degradation by the proteasome, thus accounting for the reduced steady-state levels of these AP-3 subunits in the patients' cells.

Increased Expression of Lysosomal Membrane Proteins on the Surface of AP-3-Deficient Fibroblasts

The fact that mammalian AP-3 is ubiquitously expressed (Dell'Angelica et al., 1997a; Simpson et al., 1997) led us to hypothesize that AP-3-deficient fibroblasts might display a detectable phenotype at the cellular level. Analysis of fibroblasts from patient 40 by electron microscopy indicated the presence of lysosomes of normal size and morphology; these lysosomes contained the marker proteins CD63 and lamp-1 and were accessible to internalized fluid-phase markers such as gold-conjugated bovine serum albumin (L. Hartnell and J. S. B., unpublished data). We next examined by confocal microscopy the status of various integral membrane proteins, both lysosomal (CD63, lamp-1, and lamp-2) and nonlysosomal (the transferrin receptor [TfR] and the cation-dependent mannose 6-phosphate receptor [M6PR]), whose intracellular trafficking is controlled by cytosolic sorting signals. Immunofluorescence staining of both permeabilized and nonpermeabilized fibroblasts revealed increased expression of CD63 on the surface of cells from patient 40 relative to normal cells (Figures 5A–5D and 6A). Increased levels of CD63 on the surface of the patient's fibroblasts were further evidenced by flow cytofluorometry (Figure 6C) and were also observed in B-lymphoblastoid cell lines derived from this patient as well as from patient 42 (Figure 6D). Cells derived from a heterozygous family member displayed surface CD63 levels that were comparable to those of unrelated normal individuals (Figure 6D), thus implying that the observed differences did not reflect variations in the normal population but rather a legitimate cellular phenotype associated with AP-3 deficiency. We also detected increased surface levels of lamp-1 and lamp-2 in the patient's cells by immunofluorescence staining of nonpermeabilized cells (Figure 6A), although most of these proteins still localized to internal structures and their surface expression was too low for quantitation by flow cytofluorometry (data not shown). The patient's cells also displayed increased internalization of antibodies to CD63, lamp-1, and lamp-2 (Figures 5E, 5F, and 6B) upon incubation of the cells for 15 min at 37°C. This result implied that internalization of these proteins was not defective in AP-3-deficient cells. Contrasting with the results obtained for CD63, lamp-1, and lamp-2, the distribution, surface expression, and internalization of nonlysosomal membrane proteins such as TfR and M6PR were indistinguishable in normal and patient cells (Figure 6; data not shown). Taken together, these results argue for a specific role of AP-3 in the intracellular trafficking of lysosomal integral membrane proteins.

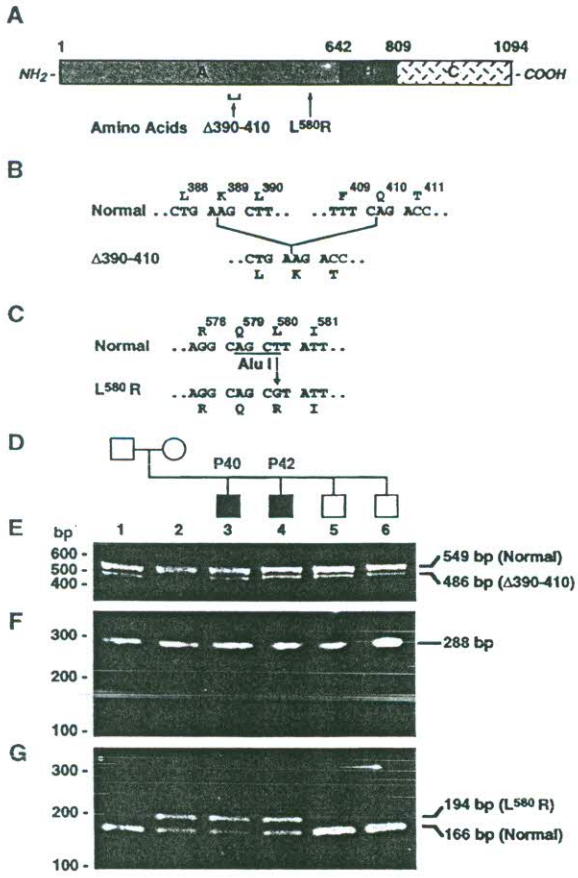

Figure 3. Mutations of the β3A Gene in HPS Patients

(A) Schematic representation of the β3A subunit of AP-3 showing the amino-terminal ("A"), hinge ("H"), and carboxy-terminal ("C") domains of the protein (Dell'Angelica et al., 1997b). The amino acid numbers demarcating the boundaries of the different regions are shown on top. The scheme also shows the approximate positions of a 21-amino acid deletion (Δ390–410) and a single amino acid substitution ($L^{580}R$) found in patients 40 and 42.

(B) Sequence of the Δ390–410 deletion allele.

(C) Sequence of the $L^{580}R$ single amino acid substitution allele indicating the position of the AluI site that is abrogated by the point mutation.

(D) Pedigree of the family of patients 40 and 42.

(E) Agarose gel electrophoretic analysis of the deletion mutation. Notice the presence of a 486 bp band corresponding to the deletion allele in the RT-PCR products obtained from the father (lane 1) and the four siblings (lanes 3–6).

(F) Agarose gel electrophoresis of a 288 bp RT-PCR product including the site of the point mutation.

(G) Agarose gel electrophoretic analysis of the fragments shown in (F) after digestion with AluI. The 194 bp fragment corresponds to the point mutated allele ($L^{580}R$), which was detected in the mother (lane 2) and patients 40 and 42 (lanes 3 and 4).

Differential Interactions of the AP-3 μ3A Subunit with the Tyrosine-Based Sorting Signals of CD63, lamp-1, and TfR

All the lysosomal and nonlysosomal membrane proteins described above contain cytosolic tyrosine-based sorting signals conforming to the sequence YXXØ (Y represents tyrosine; X, any amino acid; and Ø, a bulky hydrophobic amino acid; reviewed by Marks et al., 1997). These signals interact with the μ1, μ2, and μ3A subunits of AP-1, AP-2, and AP-3, respectively (Ohno et al., 1995, 1996). To investigate whether the differential effects of AP-3 deficiency on trafficking of lysosomal and nonlysosomal membrane proteins reflected preferential signal recognition by the μ3A subunit, we used the two-hybrid system to analyze its interaction with the tyrosine-based signals of CD63, lamp-1, and TfR. As shown in Figure 7, μ3A interacted with the signals of both CD63 and lamp-1 but not with that of TfR. We also detected interaction of μ1 with the signal of lamp-1 and of μ2 with the three signals (Figure 7). These results support the notion that AP-3 preferentially recognizes signals involved in lysosomal targeting and suggest that impairment of this function may underlie the observed misrouting of lysosomal membrane proteins in AP-3-deficient cells.

Discussion

Mutations in the β3A Locus as a Novel Cause of HPS

It has recently become evident that HPS can arise from mutations in different genetic loci, since only a subset of HPS patients have mutations in the *HPS1* gene (Hazelwood et al., 1997). In this study, we report the identification of two HPS patients with heterozygous mutations in a second locus, which encodes the β3A subunit of the AP-3 adaptor complex. The mutations consist of an internal 21-amino acid deletion and a leucine-to-arginine substitution. Both mutations occur within the β3A amino-terminal "trunk" domain, which is presumably involved in assembly with other AP-3 subunits (Dell'Angelica et al., 1997b, Simpson et al., 1997). The mutations render the β3A molecule highly susceptible to degradation in vivo, which in turn affects the stability of σ3. Although we have not performed pulse-chase analyses of the fate of μ3A and δ, the reduced steady-state levels of these proteins in the patient's cells (Figure 2A) suggest that they may undergo increased degradation as well. Degradation is likely effected by the ubiquitin–proteasome pathway, a common fate for many abnormal proteins and unassembled subunits of multiprotein complexes (Bonifacino and Weissman, 1998).

Mutations in the δ subunit of AP-3 have recently been identified as the primary defect in the mutant mouse strain *mocha* (Kantheti et al., 1998). Like the HPS patients described here, *mocha* mice display hypopigmentation and platelet dysfunction. However, *mocha* mice also exhibit neurological abnormalities, including hyperexcitability and a tendency to seizures, that are typically not observed in HPS patients. These differences are likely explained by the expression in neuronal cells of an additional isoform of β3A (termed β3B or β-NAP; Newman et al., 1995) that in these cells may compensate for the deficiency in β3A.

Altered Lysosomal Targeting in AP-3-Deficient Cells

Although the most obvious manifestations of HPS occur in specialized cell types, our studies have uncovered a sorting phenotype in cultured fibroblasts from AP-3-deficient patients. The cells displayed increased surface expression of the lysosomal membrane proteins CD63, lamp-1, and lamp-2. This phenotype was not due to

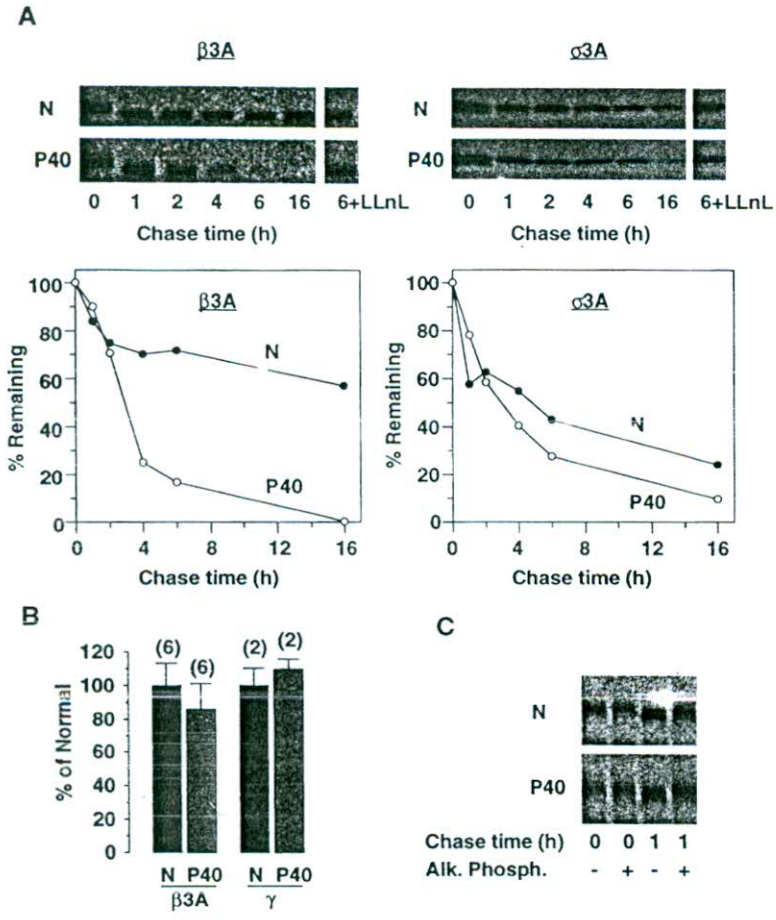

Figure 4. Enhanced Degradation of β3A and σ3A in Cultured Fibroblasts from Patient 40

(A) Cultures of normal (N) and patient 40 (P40) fibroblasts were metabolically labeled for 20 min with [^{35}S]methionine and chased for the times indicated in the figure, either in the absence or in the presence of the proteasome inhibitor LLnL (0.1 mM). Cells were detergent-solubilized under denaturing conditions and β3A and σ3A isolated by immunoprecipitation. Samples were analyzed by SDS-PAGE and fluorography, and bands were quantified by densitometric scanning. Each data point represents the mean of duplicate samples.

(B) The biosynthesis of AP-3 β3A or AP-1 γ in normal (N) and patient 40 (P40) fibroblasts labeled for 20 min was measured as described in (A) and normalized to the total amount of [^{35}S]methionine incorporated into proteins, as determined by trichloroacetic acid precipitation. The results are expressed as the mean ± SEM of the number of determinations shown in parentheses.

(C) β3A was isolated by immunoprecipitation from normal (N) and patient 40 (P40) fibroblasts pulse-labeled for 20 min and chased for 0 or 1 hr as described in (A). Immunoprecipitates were incubated in the absence or presence of alkaline phosphatase prior to analysis by SDS-PAGE. Notice the alkaline-phosphatase-induced shift in electrophoretic mobility of β3A after the 1 hr chase in both normal (N) and patient 40 (P40) fibroblasts.

impaired internalization and seemed specific for lysosomal proteins as the distribution and internalization of several nonlysosomal integral membrane proteins were not detectably altered in the AP-3-deficient cells. These observations suggest that AP-3 functions in protein targeting to lysosomes from an intracellular site.

Biochemical and morphological evidence indicates that AP-3 is a component of an organellar coat that, like other well-characterized coats, may drive formation of carrier vesicles and recruitment of cargo molecules for transport by these vesicles (Simpson et al., 1996; Dell' Angelica et al., 1997a, 1998; Faúndez et al., 1998). The missorting of CD63 and other lysosomal membrane proteins in AP-3-deficient cells could therefore reflect an essential role for the complex in vesicle formation and/or cargo selection. In this context, our results from two-hybrid analyses suggest that AP-3 is directly involved in the recognition of lysosomal targeting signals. Indeed, the μ3A subunit of the complex specifically interacted with the tyrosine-based signals of CD63 and lamp-1 but not with that of TfR. This finding is in line with a recent study showing that μ3A is the only adaptor medium chain characterized to date that prefers signals with sequence features characteristic of lysosomal targeting signals (Ohno et al., 1998). On the other hand, the μ2 subunit of the plasma membrane adaptor complex AP-2 interacted with the tyrosine-based signals of the three proteins, a result that explains the observation that internalization of CD63, lamp-1, and TfR was not impaired in fibroblasts from patient 40, which, although deficient in AP-3, had normal levels of AP-2.

Two alternative pathways for transport of newly synthesized membrane proteins to mammalian lysosomes have been proposed (reviewed by Kornfeld and Mellman, 1989; Hunziker and Geuze, 1996). One of these pathways is referred to as the "direct" route and involves transport from the TGN to an endosomal compartment from which proteins are subsequently delivered to lysosomes. The other pathway, referred to as the "indirect" route, goes from the TGN to the plasma membrane and then to endosomes and lysosomes. AP-3 could function in transport from the TGN to endosomes (i.e., in the direct route), as suggested by the proposed localization of AP-3 to the TGN (Simpson et al., 1996). According to this model, reduction of AP-3 levels would result in increased trafficking of lysosomal membrane proteins through the indirect route. Our immunofluorescence microscopy analyses of human fibroblasts, however, revealed little colocalization of AP-3 with TGN markers (E. C. D. and J. S. B., unpublished data). Rather, the majority of AP-3 in these cells was found associated with peripheral cytoplasmic structures (Figure 1), many of which contained the endosomal marker TfR (E. C. D. and J. S. B., unpublished data). This leads us to propose

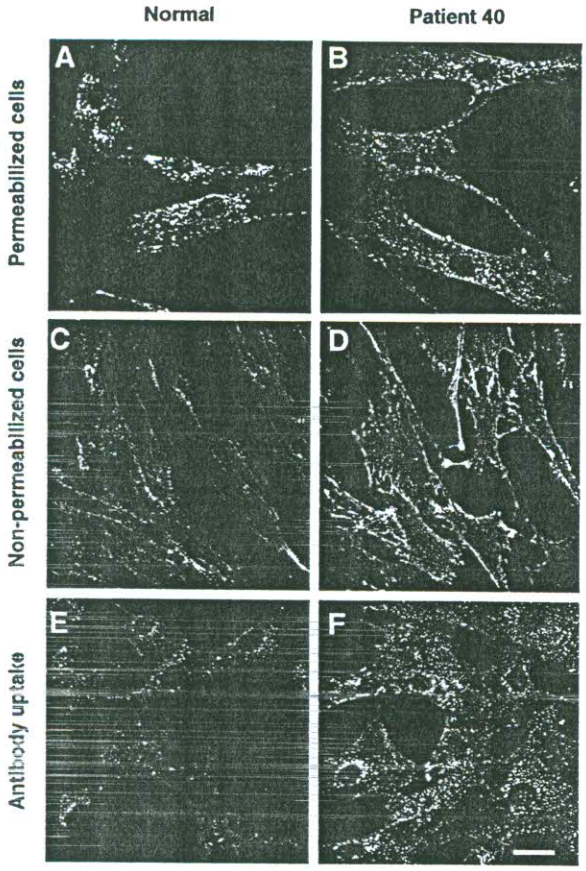

Figure 5. Increased Surface Expression of CD63 in AP-3 Deficient Cells

(A–B) Immunofluorescence microscopy analysis of the distribution of endogenous CD63 in normal (A) and patient 40 (B) fibroblasts permeabilized with saponin.

(C–D) Immunofluorescence microscopy analysis of the expression of endogenous CD63 on the surface of nonpermeabilized normal (C) and patient 40 (D) fibroblasts.

(E–F) Immunofluorescence microscopy imaging of normal (E) and patient 40 (F) fibroblasts allowed to internalize antibodies to CD63 for 15 min at 37°C. Bar, 20 μm.

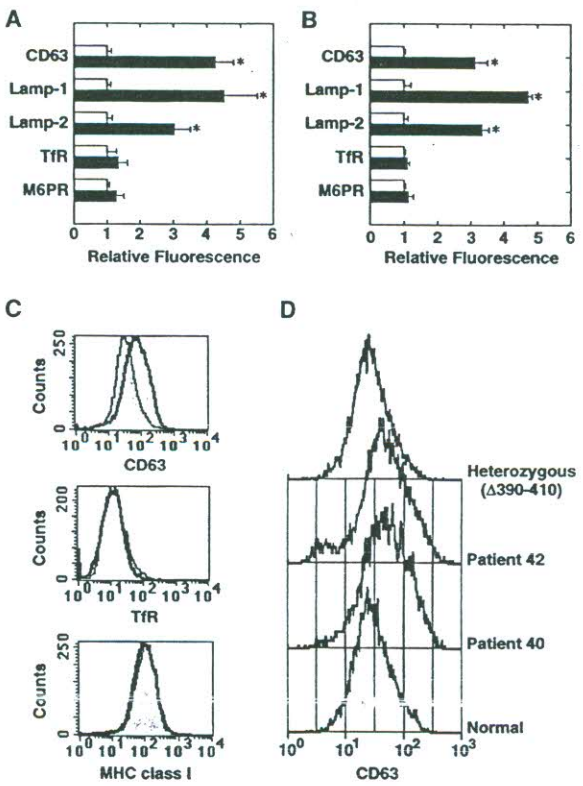

Figure 6. Differential Effects of AP-3 Deficiency on Surface Expression and Internalization of Lysosomal and Nonlysosomal Proteins

(A) Analysis of the surface expression of CD63, lamp-1, lamp-2, TfR, and M6PR in normal (empty bars) or patient 40 (solid bars) fibroblasts as determined by immunofluorescence staining of nonpermeabilized cells followed by confocal microscopy and computer-assisted image analysis. Values of fluorescence intensity per cell (mean ± SD, three independent experiments) are relative to those of normal fibroblasts. Student's t-test: *, $p < 0.05$.

(B) Quantitation of antibody internalization experiments by computer-assisted measurement of the fluorescence per cell of samples prepared as in Figures 5E and 5F. Values are relative to those obtained for the normal control and represent means ± S. D. of three independent experiments. Student's t-test: *, $p < 0.05$.

(C) Flow cytometric analysis of the expression of CD63, TfR, and MHC class I molecules on the surface of fibroblasts from a normal individual (thin, filled curve) and patient 40 (thick, unfilled curve).

(D) Flow cytometric analysis of the expression of CD63 in B-lymphoblastoid cell lines from a normal individual, patients 40 and 42, and the patients' father (heterozygous Δ390–410).

an alternative model in which AP-3 functions in the recruitment of proteins for transport to lysosomes from an endosomal compartment. Proteins having pure endocytic signals (e.g., the TfR) would not be recognized by AP-3 and would thus be directed to the plasma membrane. This second model is consistent with a recent in vitro study showing AP-3-mediated formation of vesicles that excluded TfR from purified endosomal membranes (Lichtenstein et al., 1998). According to this model, depletion of AP-3 would compromise the targeting of lysosomal membrane proteins from endosomes, this in turn leading to a buildup of these proteins in a plasma membrane-endosome recycling circuit. The consequences of AP-3 deficiency would thus be similar to those of mutating a glycine before the critical tyrosine in the signal from lamp-1 (Harter and Mellman, 1992) or changing the spacing of the lamp-1 signal relative to the transmembrane domain (Rohrer et al., 1996), manipulations that result in increased delivery of the protein to the plasma membrane and cycling between this compartment and endosomes.

Role of AP-3 in the Biogenesis of Melanosomes and Platelet-Dense Granules

The altered trafficking of lysosomal membrane proteins in fibroblasts and B-lymphoblastoid cell lines suggests a likely explanation for the abnormalities in melanosomes and platelet-dense granules in AP-3-deficient patients. Melanosomal membrane proteins such as tyrosinase, TRP1, and TRP2 contain tyrosine- or dileucine-based sorting signals similar to those found in lysosomal membrane proteins (Vijayasaradhi et al., 1995; reviewed by Odorizzi et al., 1998). Indeed, the dileucine-based signal of tyrosinase has been shown to interact with AP-3 in

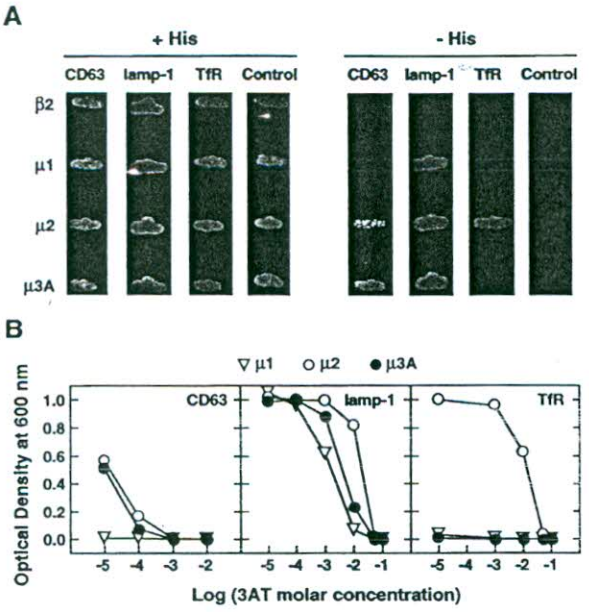

Figure 7. Yeast Two-Hybrid Analysis of the Interaction of the Sorting Signals of CD63, lamp-1, and TfR with Different Adaptor Subunits

GAL4 transcription activation domain fused to β2, μ1, μ2, or μ3A were coexpressed in yeast cells with GAL4 DNA-binding domain fused to a TGN38 tail-derived segment bearing either an inactive sequence (SDAQRL, control) or the tyrosine-based sorting signals of CD63 (SGYEVM), lamp-1 (AGYQTI), or TfR (LSYTRF).

(A) Plate growth assay. Yeast cells were plated on minimal medium plates with (+His) or without (−His) histidine. Interactions were detected based on the ability of the cotransformed yeast cells to grow in the absence of histidine.

(B) Growth inhibition assay. Interactions between the μ subunits and the signals of CD63, lamp-1, and TfR were further characterized by measuring growth of the cotransformed yeast cells after 2 days of culture in a minimal liquid medium lacking histidine and containing different concentrations of the histidine biosynthesis inhibitor 3-amino-1,2,4-triazole (3AT), as described (Aguilar et al., 1997).

vitro (Höning et al., 1998). Much less is known about integral membrane proteins that are specific to the membrane of platelet-dense granules. We anticipate, however, that some of these proteins will contain the same type of generic sorting signals present in lysosomal and melanosomal integral membrane proteins. Thus, AP-3 could be involved in sorting some or all of these proteins to their specific organelles from the same site where lysosomal membrane proteins are sorted to lysosomes (i.e., the TGN or endosomes). A prediction of this model is that absence of AP-3 would result in increased expression of the organelle-specific proteins at the cell surface. There are other specialized cytoplasmic organelles that contain organelle-specific as well as lysosomal proteins; these include lytic granules (Bonifacino et al., 1989) and MHC class II antigen-processing compartments (Peters et al., 1991; Marks et al., 1995). It will now be of interest to determine if these organelles are also abnormal in AP-3-deficient patients.

Concluding Remarks

The results presented here clearly implicate the mammalian AP-3 complex in the trafficking of lysosomal membrane proteins. AP-3 function thus appears to be conserved among eukaryotes, since there is also compelling evidence for a role of yeast AP-3 in signal-mediated protein transport to the vacuole, the equivalent of mammalian lysosomes (Cowles et al., 1997, Stepp et al., 1997; Darsow et al., 1998; Vowels and Payne, 1998). The presence of a significant amount of lysosomal membrane proteins in lysosomes of AP-3-deficient cells, however, suggests the existence of additional, AP-3-independent pathways for lysosomal targeting. The availability of AP-3 deficient cells should now allow further studies of these alternative pathways. In addition, the identification of other genes that cause HPS in humans, or related disorders in mice and *Drosophila*, should eventually help to delineate the molecular machinery involved in lysosome biogenesis in higher eukaryotes.

Experimental Procedures

Patients and Cell Culture

The patients involved in this study were enrolled in a protocol approved by the NICHD Institutional Review Board, and all of them or their parents provided written informed consent. HPS was diagnosed on the basis of oculocutaneous albinism and by the absence of platelet-dense granules on electron microscopy. Two patients were homozygous for a 16 bp duplication in exon 15 of the *HPS1* gene (Oh et al., 1996), while the remaining 18 patients (from 16 families) had a normal-sized transcript and no discernible mutations in *HPS1* as judged by single strand conformational polymorphism screening followed by sequencing of suspicious regions. Patient numbers correspond to those of a master file of all NICHD patients with HPS. Primary cultures of skin fibroblasts were cultured in Dulbecco's modified Eagle's medium (DMEM) supplemented with 20% (v/v) fetal bovine serum, 100 U/ml penicillin, and 0.1 mg/ml streptomycin. Epstein-Barr virus-transformed B-lymphoblasts were propagated in RPMI 1640 medium containing 9% (v/v) fetal bovine serum, 100 U/ml penicillin, and 0.1 mg/ml streptomycin.

Antibodies

The preparation and characterization of the following rabbit antibodies to AP-3 subunits have been described elsewhere: anti-μ3 (anti-p47) and anti-σ3 (Dell'Angelica et al., 1997a), β3A1 and β3C1 antibodies to β3A (Dell'Angelica et al., 1997b), and anti-δ (Ooi et al., 1998). Goat antiserum to human M6PR was kindly provided by Drs. T. Braulke and K. Von Figura (University of Göttingen, Germany). The following commercially available monoclonal antibodies were used: 100/2 anti-α-adaptin and 100/3 anti-γ-adaptin (Sigma Chemical Co., St. Louis, MO); B3/25 anti-TfR (Boehringer Mannheim, Indianapolis, IN); H4A3 anti-lamp-1, H4B4 anti-lamp-2, and H5C6 anti-CD63 (Developmental Studies Hybridoma Bank at the University of Iowa, Iowa City, IO); 1D9 anti-ARF and AP.6 anti-α-adaptin (Affinity Bioreagents, Golden, CO); fluorescein-conjugated anti-CD63 and anti-TfR (Coulter/Immunotech, Marseille Cedex, France), and fluorescein-conjugated anti-MHC class I (Pharmingen, San Diego, CA). Cy3-conjugated secondary antibodies were from Jackson Immunoresearch (West Grove, PA), and Alexa 448-conjugated antibodies were from Molecular Probes (Eugene, OR).

Nucleic Acid Isolation and Sequencing

RNA and DNA were purified from peripheral blood using the Purescript and Puregene kits, respectively (Gentra Systems, Minneapolis, MN). Total RNA from cultured fibroblasts was isolated by using the TRIzol reagent (GIBCO BRL-Life Technologies, Gaithersburg, MD). The sequence of the coding regions of the AP-3 subunits δ, β3A, μ3A, μ3B, σ3A, and σ3B was determined by RT-PCR amplification of overlapping segments (0.5–1.2 kb) followed by gel-purification and direct cycle sequencing. The sequences of the primers used for RT-PCR and sequencing are available upon request. The sequences obtained for patients 40 and 42 were compared to those of human δ (Ooi et al., 1997), β3A (Dell'Angelica et al., 1997b), μ3B

(Koyama et al., 1995), σ3A (Watanabe et al., 1996; Dell'Angelica et al., 1997a; Simpson et al., 1997), σ3B (Dell'Angelica et al., 1997a), and μ3A.

Northern Blot Analysis

The generation of probes for δ, β3A, σ3A, and σ3B mRNAs has been described elsewhere (Dell'Angelica et al., 1997a, 1997b; Ooi et al., 1997). The μ3A and μ3B probes comprised their complete open reading frames and were obtained by RT-PCR and characterized by DNA sequencing. Northern blot analysis was carried out as described (Dell'Angelica et al., 1997a).

Genotype Analysis

Two PCR-based assays were used to detect the presence of specific mutations in the AP-3 β3A subunit. The first assay involved RT-PCR amplification of nucleotides 826–1374 of the human β3A mRNA (GenBank accession number U81504), which allowed detection of the Δ390–410 deletion as a PCR product that is 63 bases shorter than the normal 549 bp product. The second assay was designed to detect the $L^{580}R$ mutation that originates from a G→T substitution within an AluI site; the assay consisted of RT-PCR amplification of nucleotides 1635–1922 of the human β3A mRNA and subsequent digestion with AluI, resulting in major fragments of 166 and 194 bp for the normal and mutated β3A forms, respectively. Primer sequences and RT-PCR conditions are available upon request.

Pulse-Chase Experiments

Fibroblasts grown to confluence were detached from plates by trypsinization, collected by centrifugation, and then washed twice with methionine-free DMEM containing 0.1% (w/v) bovine serum albumin (BSA) and 25 mM HEPES buffer (pH 7.4). Washed cells were resuspended in 3 ml of the above medium containing 1 Ci/l of [^{35}S]methionine (Express Protein Label, Dupont-New England Nuclear, Boston, MA) and then incubated for 20 min at 37°C. Subsequently, cells were collected by centrifugation, resuspended in DMEM containing 9% (v/v) fetal bovine serum and 25 mM HEPES (pH 7.4), and divided into aliquots that were either frozen immediately on dry ice (0 hr chase) or incubated at 37°C for different chase periods (1–16 hr) before freezing. The resulting samples were analyzed by denaturing immunoprecipitation (Bonifacino and Dell'Angelica, 1998) using the anti-σ3, anti-γ-adaptin (100/3), and anti-β3A (β3C1) antibodies. The immunoprecipitates obtained using the β3C1 antibody were subjected to a second immunoprecipitation (recapture) step (Bonifacino and Dell'Angelica, 1998) with the same antibody in order to reduce the background. Immunoprecipitates were analyzed by SDS-PAGE followed by fluorography, and band intensities were quantified by densitometric scanning.

Other Biochemical Procedures

Immunoblot analysis of whole-cell extracts was carried out as described previously (Dell'Angelica et al., 1997a). For gel filtration analysis, fibroblast lysates were prepared by incubating the cells on ice for 15 min in 0.1 M Tris-HCl buffer (pH 7.5) containing 1% (w/v) Triton X-100, 10 mM EDTA, 2 mM AEBSF, 20 mg/l aprotinin, 4 ml/l leupeptin, and 2 mg/l pepstatin A. The lysates were diluted with an equal volume of 1 M Tris-HCl (pH 7.5), incubated for 15 min at 4°C, and then centrifuged at 16,000 × g for 15 min at 4°C. The cleared lysates (0.2 ml, ~0.6 mg protein) were fractionated on a Superose 6 HR 10/30 column (Pharmacia Biotech, Uppsala, Sweden), equilibrated, and eluted at 4°C with 0.5 M Tris-HCl (pH 7.5), 0.5% (w/v) Triton X-100, 5 mM EDTA, 1 mM AEBSF, at a flow rate of 0.4 ml/min. Fractions (0.4 ml) were collected and analyzed by immunoblotting.

Immunofluorescence

Indirect immunofluorescence of fixed, permeabilized cells was carried out as described (Dell'Angelica et al., 1997a). For surface staining, cells grown on glass coverslips were incubated on ice for 30 min in the presence of primary antibody diluted in phosphate-buffered saline (PBS) containing 1% (w/v) BSA (PBS-BSA), washed for 5 min in ice-cold PBS, and incubated for an additional 30 min on ice in the presence of an appropriate Cy3-conjugated secondary antibody (in PBS-BSA). Cells were then washed in ice-cold PBS for 5 min, fixed with 2% formaldehyde in PBS for 10 min, and then mounted onto glass slides with Fluoromount G (Southern Biotechnologies, Birmingham, AL).

Antibody Internalization Assay

Fibroblasts grown on glass coverslips were incubated for 15 min at 37°C in the presence of primary antibodies diluted in DMEM, 1% (w/v) BSA, and 25 mM HEPES buffer (pH 7.4). Subsequently, cells were washed either for 5 min in ice-cold PBS (for antibodies to lamp-1 or lamp-2) or for 5 min in 0.2 M acetate buffer (pH 2.4), 0.5 M NaCl at 4°C followed by 2 min in ice-cold PBS (for antibodies to CD63, TfR, or M6PR). Washed cells were fixed in 2% formaldehyde for 10 min, incubated for 1 hr at room temperature in the presence of Cy3-conjugated secondary antibody (diluted in PBS, 0.1% [w/v] BSA, 0.1% [w/v] saponin), rinsed with PBS, and then mounted onto glass slides with Fluoromount G.

Confocal Microscopy

Fluorescence images were acquired on a Zeiss LSM 410 confocal microscope (Carl Zeiss Inc., Thornwood, NY) using identical parameters for normal and patient cells. For quantitation, five randomly selected fields (containing 14 ± 7 cells per field) were imaged avoiding signal saturation, and the average fluorescence per cell was calculated by using the NIH image 1.62/ppc program. Values were corrected for background fluorescence, normalized to those obtained for normal control cells, and expressed as mean ± SD of three independent experiments.

Flow Cytometry

Fibroblasts were detached from plates by incubation at 37°C for 15 min in the presence of PBS-BSA containing 20 mM EDTA, followed by gentle scraping. Cells were passed through a 70 μm filter, collected by centrifugation, and then washed twice with ice-cold PBS-BSA. Cultured B-lymphoblasts were harvested by centrifugation and washed twice with RPMI medium containing 1% (v/v) fetal bovine serum and 25 mM HEPES buffer (pH 7.4) (RPMI-FBS-HEPES). Approximately 5×10^5 cells were incubated for 30 min on ice in the presence of fluorescein-conjugated antibodies diluted in 0.1 ml of either PBS-BSA (for fibroblasts) or RPMI-BFS-HEPES (for lymphoblasts). Subsequently, cells were washed first with 3 ml of either PBS-BSA (fibroblasts) or RPMI-BFS-HEPES (lymphoblasts) and then with 3 ml of PBS. The final cell pellet was resuspended in PBS for analysis on a FACScan flow cytometer (Becton Dickinson, Mountain View, CA).

Two-Hybrid Assays

The two-hybrid constructs GAL4bd-TGN38 Tail Δ1 (Y→A), GAL4bd-TGN38 Tail Δ1 (SDYQRL→LSYTRF), GAL4bd-TGN38 Tail Δ1 (SDYQRL→AGYQTI), GAL4ad-μ1, GAL4ad-μ2, GAL4ad-μ3A, and GAL4ad-β2 have been described previously (Ohno et al., 1995, 1996; Aguilar et al., 1997). The construct GAL4bd-TGN38 Tail Δ1 (SDYQRL→SGYEVM) was prepared by ligating synthetic oligonucleotides into the EagI-PstI sites of GAL4bd-TGN38 Tail Δ1 (Ohno et al., 1996). Transformation of *Saccharomyces cerevisiae* strain HF7c with the above constructs and subsequent growth assays were carried out as described previously (Aguilar et al., 1997).

Acknowledgments

We thank Lisa Hartnell for electron microscopy analyses, Tim LaVaute for help with preparation of B-lymphoblastoid cell lines and with flow cytofluorometry, John Presley for advice on image analysis, Jennifer Lippincott-Schwartz, John Hammer, and Chris Mullins for critical reading of the manuscript, and the patients and their families for their cooperation.

Received October 12, 1998; revised November 25, 1998.

References

Aguilar, R.C., Ohno, H., Roche, K.W., and Bonifacino, J.S. (1997). Functional domain mapping of the clathrin-associated adaptor medium chains μ1 and μ2. J. Biol. Chem. 272, 27160–27166.

Bonifacino, J.S., and Dell'Angelica, E.C. (1998). Immunoprecipitation. In Current Protocols in Cell Biology, J.S. Bonifacino, M. Dasso, J.B. Harford, J. Lippincott-Schwartz, and K. Yamada, eds. (New York: John Wiley and Sons), pp. 7.2.1–7.2.21.

Bonifacino, J.S., and Weissman, A.M. (1998). Ubiquitin and the control of protein fate in the secretory and endocytic pathways. Annu. Rev. Cell Dev. Biol. *14*, 19–57.

Bonifacino, J.S., Yuan, L., and Sandoval, I.V. (1989). Internalization and recycling to serotonin-containing granules of the 80K integral membrane protein exposed on the surface of secreting rat basophilic leukaemia cells. J. Cell Sci. *92*, 701–712.

Cowles, C.R., Odorizzi, G., Payne, G.S., and Emr, S.D. (1997). The AP-3 adaptor complex is essential for cargo-selective transport to the yeast vacuole. Cell *91*, 109–118.

Darsow, T., Burd, C.G., and Emr, S.D. (1998). Acidic di-leucine motif essential for AP-3-dependent sorting and restriction of the functional specificity of the Vam3p vacuolar t-SNARE. J. Cell Biol. *142*, 913–922.

Davis, C.G., Lehrman, M.A., Russell, D.W., Anderson, R.G., Brown, M.S., and Goldstein, J.L. (1986). The J.D. mutation in familial hypercholesterolemia: amino acid substitution in cytoplasmic domain impedes internalization of LDL receptors. Cell *45*, 15–24.

Dell'Angelica, E.C., Ohno, H., Ooi, C.E., Rabinovich, E., Roche, K.W., and Bonifacino, J.S. (1997a). AP-3: an adaptor-like protein complex with ubiquitous expression. EMBO J. *16*, 917–928.

Dell'Angelica, E.C., Ooi, C.E., and Bonifacino, J.S. (1997b). β3A-adaptin, a subunit of the adaptor-like complex AP-3. J. Biol. Chem. *272*, 15078–15084.

Dell'Angelica, E.C., Klumperman, J., Stoorvogel, W., and Bonifacino, J.S. (1998). Association of the AP-3 adaptor complex with clathrin. Science *280*, 431–434.

Faúndez, V., Horng, J.-T., and Kelly, R.B. (1998). A function for the AP3 coat complex in synaptic vesicle formation from endosomes. Cell *93*, 423–432.

Harter, C., and Mellman, I. (1992). Transport of the lysosomal membrane glycoprotein lgp120 (lgp-A) to lysosomes does not require appearance on the plasma membrane. J. Cell Biol. *117*, 311–325.

Hazelwood, S., Shotelersuk, V., Wildenberg, S.C., Chen, D., Iwata, F., Kaiser-Kupfer, M.I., White, J.G., King, R.A., and Gahl, W.A. (1997). Evidence for locus heterogeneity in Puerto Ricans with Hermansky-Pudlak syndrome. Am. J. Hum. Genet. *61*, 1088–1094.

Hermansky, F., and Pudlak, P. (1959). Albinism associated with hemorrhagic diathesis and unusual pigmented reticular cells in the bone marrow; report of two cases with histochemical studies. Blood *14*, 162–169.

High, S., and Laird, V. (1997). Membrane protein biosynthesis all sewn up? Trends Cell. Biol. *7*, 206–210.

Höning, S., Sandoval, I.V., and von Figura, K. (1998). A di-leucine-based motif in the cytoplasmic tail of LIMP-II and tyrosinase mediates selective binding of AP-3. EMBO J. *17*, 1304–1314.

Hunziker, W., and Geuze, H.J. (1996). Intracellular trafficking of lysosomal membrane proteins. Bioessays *18*, 379–389.

Israels, S.J., McMillan, E.M., Robertson, C., Singhory, S., and McNicol, A. (1996). The lysosomal granule membrane protein, LAMP-2, is also present in platelet dense granule membranes. Thromb. HaemosL *75*, 623–629.

Jensen, T.J., Loo, M.A., Pind, S., Williams, D.B., Goldberg, A.L., and Riordan, J.R. (1995). Multiple proteolytic systems, including the proteasome, contribute to CFTR processing. Cell *83*, 129–135.

Kantheti, P., Qiao, X., Diaz, M.E., Peden, A.A., Meyer, G.E., Carskadon, S.L., Kapfhamer, D., Sufalko, D., Robinson, M.S., Noebels, J.L., and Burmeister, M. (1998). Mutation in AP-3 delta in the mocha mouse links endosomal transport to storage deficiency in platelets, melanosomes, and synaptic vesicles. Neuron *21*, 111–122.

Kirchhausen, T., Bonifacino, J.S., and Riezman, H. (1997). Linking cargo to vesicle formation: receptor tail interactions with coat proteins. Curr. Opin. Cell Biol. *9*, 488–495.

Kornfeld, S., and Mellman, I. (1989). The biogenesis of lysosomes. Annu. Rev. Cell Biol. *5*, 483–525.

Koyama, K., Sudo, K., and Nakamura, Y. (1995). Isolation of 115 human chromosome 8-specific expressed-sequence tags by exon amplification. Genomics *26*, 245–253.

Lichtenstein, Y., Desnos, C., Faúndez, V., Kelly, R.G., and Clift-O'Grady, L. (1998). Vesiculation and sorting from PC12-derived endosomes in vitro. Proc. Natl. Acad. Sci. USA *95*, 11223–11228.

Marks, M.S., Roche, P.A., van Donselaar, E., Woodruff, L., Peters, P.J., and Bonifacino, J.S. (1995). A lysosomal targeting signal in the cytoplasmic tail of the β chain directs HLA-DM to MHC class II compartments. J. Cell Biol. *131*, 351–369.

Marks, M.S., Ohno, H., Kirchhausen, T., and Bonifacino, J.S. (1997). Protein sorting by tyrosine-based signals: adapting to the Ys and wherefores. Trends Cell Biol. *7*, 124–128.

Newman, L.S., McKeever, M.O., Okano, H.J., and Darnell, R.B. (1995). Beta-NAP, a cerebellar degeneration antigen, is a neuron-specific vesicle coat protein. Cell *82*, 773–783.

Odorizzi, G., Cowles, C.R., and Emr, S.D. (1998). The AP-3 complex: a coat of many colours. Trends Cell Biol. *8*, 282–288.

Oh, J., Bailin, T., Fukai, K., Feng, G.H., Ho, L., Mao, J.I., Frenk, E., Tamura, N., and Spritz, R.A. (1996). Positional cloning of a gene for Hermansky-Pudlak syndrome, a disorder of cytoplasmic organelles. Nat. Genet. *14*, 300–306.

Ohno, H., Stewart, J., Fournier, M.C., Bosshart, H., Rhee, I., Miyatake, S., Saito, T., Gallusser, A., Kirchhausen, T., and Bonifacino, J.S. (1995). Interaction of tyrosine-based sorting signals with clathrin-associated proteins. Science *269*, 1872–1875.

Ohno, H., Fournier, M.C., Poy, G., and Bonifacino, J.S. (1996). Structural determinants of interaction of tyrosine-based sorting signals with the adaptor medium chains. J. Biol. Chem. *271*, 29009–29015.

Ohno, H., Aguilar, R.C., Yeh, D., Taura, D., Saito, T., and Bonifacino, J.S. (1998). The medium subunits of adaptor complexes recognize distinct but overlapping sets of tyrosine-based sorting signals. J. Biol. Chem. *273*, 25915–25921.

Ooi, C.E., Moreira, J.E., Dell'Angelica, E.C., Poy, G., Wassarman, D.A., and Bonifacino, J.S. (1997). Altered expression of a novel adaptin leads to defective pigment granule biogenesis in the *Drosophila* eye color mutant *garnet*. EMBO J. *16*, 4508–4518.

Ooi, C.E., Dell'Angelica, E.C., and Bonifacino, J.S. (1998). ADP-ribosylation factor 1 (ARF1) regulates recruitment of the AP-3 adaptor complex to membranes. J. Cell Biol. *142*, 391–402.

Orlow, S.J. (1995). Melanosomes are specialized members of the lysosomal lineage of organelles. J. Invest. Dermatol. *105*, 3–7.

Peters, P.J., Neefjes, J.J., Oorschot, V., Ploegh, H.L., and Geuze, H.J. (1991). Segregation of MHC class II molecules from MHC class I molecules in the Golgi complex for transport to lysosomal compartments. Naturo *349*, 669–676.

Pevsner, J., Volknandt, W., Wong, B.R., and Scheller, R.H. (1994). Two rat homologs of clathrin-associated adaptor proteins. Gene *146*, 279–283.

Rohrer, J., Schweizer, A., Russell, D., and Kornfeld, S. (1996). The targeting of Lamp1 to lysosomes is dependent on the spacing of its cytoplasmic tail tyrosine sorting motif relative to the membrane. J. Cell Biol. *132*, 565–576.

Rothman, J.E., and Wieland, F.T. (1996). Protein sorting by transport vesicles. Science *272*, 227–234.

Schekman, R., and Orci, L. (1996). Coat proteins and vesicle budding. Science *271*, 1526–1533.

Simpson, F., Bright, N.A., West, M.A., Newman, L.S., Darnell, R.B., and Robinson, M.S. (1996). A novel adaptor-related protein complex. J. Cell Biol. *133*, 749–760.

Simpson, F., Peden, A.A., Christopoulou, L., and Robinson, M.S. (1997). Characterization of the adaptor-related protein complex, AP-3. J. Cell Biol. *137*, 835–845.

Stopp, J.D., Huang, K., and Lemmon, S.K. (1997). The yeast AP-3 complex is essential for the efficient delivery of alkaline phosphatase by the alternate pathway to the vacuole. J. Cell Biol. *139*, 1761–1774.

Vijayasaradhi, S., Xu, Y., Bouchard, B., and Houghton, A.N. (1995). Intracellular sorting and targeting of melanosomal membrane proteins: identification of signals for sorting of the human brown locus protein, gp75. J. Cell Biol. *130*, 807–820.

Vowels, J.J., and Payne, G.S. (1998). A dileucine-like sorting signal directs transport into an AP-3-dependent, clathrin-independent pathway to the yeast vacuole. EMBO J *17*, 2482–2493.

Ward, C.L., Omura, S., and Kopito, R.R. (1995). Degradation of CFTR by the ubiquitin-proteasome pathway. Cell *83*, 121–127.

Watanabe, T.K., Shimizu, F., Nagata, M., Takaichi, A., Fujiwara, T., Nakamura, Y., Takahashi, E., and Hirai, Y. (1996). Cloning, expression pattern and mapping to 12p 13.2 → p13.1 of CLAPS3, a gene encoding a novel clathrin-adaptor small chain. Cytogenet. Cell Genet. *73*, 214–217.

GenBank Accession Number

The human μ3A cDNA sequence has been deposited in Genbank with the accession number AF092092.